

Primordial Black Holes (PBHs) and The Signatures of Cosmic Non-Gaussianity

Owais Farooq¹, Romana Zahoor², and Balungi Francis³

^{1,2}Department of Physics, Central University of Kashmir, Ganderbal(191131) India
 owai24831@outlook.com , romananaeem033@gmail.com, balungif@gmail.com

September 16, 2025

Abstract

Primordial black holes (PBHs) provide a unique probe of the small-scale primordial Universe and may constitute a fraction of the dark matter. Their formation is highly sensitive to non-Gaussian features in the primordial curvature perturbation ζ . In this work we investigate PBH production in the curvaton scenario, where the decay of a late-time light scalar field imprints large, inherently non-Gaussian fluctuations on small scales. Using the exact non-linear mapping between the Gaussian curvaton field perturbations and ζ , we compute the full non-perturbative probability distribution functions of ζ and derive the PBH formation fraction β without relying on a truncated non-Gaussian expansion. We show that the enhanced tail of the distribution dramatically amplifies PBH production, leading to an exponential sensitivity of β to the curvaton decay fraction $\Omega_{\chi, \text{dec}}$. By modeling the scale dependence of curvaton fluctuations with a lognormal profile, we obtain realistic, extended PBH mass spectra rather than monochromatic peaks. We further highlight the associated stochastic gravitational-wave background induced at second order, whose peak frequency correlates directly with the PBH mass scale. Our results demonstrate that the curvaton scenario naturally produces a rich phenomenology of PBHs and gravitational waves, sharply distinct from Gaussian single-field inflation models, and provide a framework for connecting small-scale non-Gaussian physics to upcoming gravitational-wave and PBH observations.

Keywords:

Non-Gaussianity, PBH's , Perturbations , inflation , kurtosis, Bispectrum, Probability distribution function(PDF)...

1 Introduction

Primordial black holes (PBHs) are black holes hypothesised to have formed in the early Universe from the collapse of overdense regions seeded by primordial curvature perturbations [8, 17, 21]. Although PBHs have not yet been observed, their possible existence has profound implications: they can serve as probes of small-scale cosmological fluctuations that are otherwise inaccessible, they may constitute a significant fraction of dark matter [6, 7], and they could provide seeds for supermassive black holes observed at high redshift [3].

The abundance of PBHs is extremely sensitive to the statistics of primordial fluctuations. In the standard picture of single-field slow-roll inflation, the curvature perturbations are nearly Gaussian, with a nearly scale-invariant power spectrum of amplitude $P_\zeta \sim 10^{-9}$ on cosmic microwave background (CMB) scales [12]. However, PBH formation requires fluctuations with amplitudes several orders of magnitude larger, $P_\zeta \sim 10^{-2}$, on

much smaller scales [16]. Such enhancements are achievable in models with features in the inflationary potential, secondary phases of inflation, or spectator/curvaton fields [5, 15, 23].

Because PBHs form from the collapse of rare, large fluctuations in the extreme tail of the probability distribution function (PDF), their formation rate is highly sensitive not only to the power spectrum amplitude but also to the presence of primordial non-Gaussianity. Even a small departure from Gaussianity can enhance or suppress the tail of the PDF, leading to exponential changes in the predicted PBH abundance [5, 34, 36]. The sign and magnitude of the non-linearity parameters ($f_{\text{NL}}, g_{\text{NL}}, \dots$) are especially important, as they determine whether the tails of the PDF are enhanced or diminished.

Multi-field models, such as the curvaton scenario, provide natural settings in which strong non-Gaussianity arises. In the curvaton model, a light scalar field generates the primordial fluctuations and can yield a highly non-Gaussian distribution whose full non-linear PDF is calculable [32, 36]. Other scenarios, such as axion-like spectator fields or hybrid inflation with waterfall transitions, can also produce strongly non-Gaussian perturbations [1, 22]. These scenarios have attracted renewed interest due to their potential to explain gravitational wave signals observed by pulsar timing arrays (PTAs) [11] and the population of merging black holes observed by LIGO-Virgo-KAGRA [10].

In this work, we investigate the implications of non-Gaussianity in multi-field inflationary scenarios for PBH production. We emphasise how different forms of non-Gaussian statistics affect the PBH mass spectrum, the associated constraints from induced gravitational waves, and the viability of PBHs as dark matter. Our analysis builds upon earlier studies of PBHs in non-Gaussian universes [5, 36], but we extend the discussion to highlight observationally relevant scenarios in light of current gravitational-wave and PTA data.

2 PBHs in a Gaussian Universe

Primordial black holes (PBHs) are expected to form when large curvature perturbations re-enter the Hubble horizon during the radiation-dominated era, causing gravitational collapse if they exceed a critical threshold [8, 17, 30, 31]. The criterion for collapse is typically expressed in terms of the density contrast at horizon crossing, $\delta_{\text{hor}}(R)$, or equivalently the curvature perturbation ζ . Numerical simulations suggest that PBHs form when the smoothed density contrast exceeds a threshold $\delta_c \sim 0.4\text{--}0.5$ [18, 29], corresponding to a critical curvature perturbation $\zeta_c \sim 0.7\text{--}1.2$, depending on the shape of the perturbation profile [19, 35]. For simplicity, many works adopt $\zeta_c \approx 1$.

The initial mass fraction of the Universe collapsing into PBHs at the time of formation is given by

$$\beta(M) \equiv \left. \frac{\rho_{\text{PBH}}}{\rho_{\text{tot}}} \right|_{\text{formation}} \simeq \int_{\zeta_c}^{\infty} P(\zeta) d\zeta, \quad (1)$$

where $P(\zeta)$ is the probability distribution function (PDF) of the curvature perturbation ζ . In the Gaussian case, this PDF is

$$P_G(\zeta) = \frac{1}{\sqrt{2\pi\sigma^2}} \exp\left(-\frac{\zeta^2}{2\sigma^2}\right), \quad (2)$$

where $\sigma^2 = \langle \zeta^2 \rangle$ is the variance, related to the power spectrum of primordial fluctuations.

Substituting (2) into (1), one obtains

$$\beta(M) \simeq \frac{1}{2} \text{erfc}\left(\frac{\zeta_c}{\sqrt{2\sigma^2}}\right), \quad (3)$$

where $\text{erfc}(x)$ is the complementary error function. Since PBHs form from extremely rare fluctuations in the far tail of the distribution, the abundance depends exponentially on ζ_c^2/σ^2 . Even a small change in σ leads to an exponential change in $\beta(M)$.

For a typical choice of $\zeta_c = 1$, if the desired mass fraction is $\beta \sim 10^{-20}$ (relevant for asteroid-mass PBHs surviving to the present epoch), then the required variance is $\sigma \simeq 0.11$. For a much larger fraction $\beta \sim 10^{-5}$, the required variance is $\sigma \simeq 0.23$ [16, 36]. These numbers illustrate that PBH formation requires σ values orders of magnitude larger than the variance on CMB scales ($\sigma \sim 10^{-5}$).

The variance σ^2 is directly related to the dimensionless power spectrum $P_\zeta(k)$ of curvature perturbations smoothed on a scale $R \sim 1/k$:

$$\sigma^2(R) = \int W^2(kR) P_\zeta(k) \frac{dk}{k}, \quad (4)$$

where $W(kR)$ is a smoothing window function, often taken to be Gaussian or a real-space top-hat [21, 36]. The horizon mass associated with scale k determines the PBH mass:

$$M(k) \simeq \gamma M_H(k) \simeq \gamma \frac{4\pi}{3} \rho H^{-3}, \quad (5)$$

where M_H is the horizon mass, H is the Hubble parameter at horizon re-entry, and $\gamma \sim 0.2$ is an efficiency factor determined from numerical collapse simulations [29, 31].

In summary, in a Gaussian universe the PBH formation rate is exponentially suppressed, requiring an unusually large small-scale power spectrum ($P_\zeta \sim 10^{-2}$) to achieve any significant abundance. This fact makes PBHs a sensitive probe of small-scale primordial fluctuations and motivates the study of non-Gaussian statistics, which can substantially alter the abundance prediction.

3 PBHs and Local Non-Gaussianity

While the Gaussian approximation provides a useful baseline for estimating primordial black hole (PBH) abundances, it is generally inadequate in multi-field inflationary scenarios, where non-linear field dynamics naturally generate non-Gaussian curvature perturbations. Since PBH formation is governed by the extreme tail of the probability distribution function (PDF), even small levels of non-Gaussianity can dramatically alter the expected PBH abundance [4, 5, 20, 36].

A common approach to model non-Gaussianity is to expand the primordial curvature perturbation ζ as a local function of an underlying Gaussian field ζ_G :

$$\zeta = \zeta_G + \frac{3}{5} f_{\text{NL}} (\zeta_G^2 - \langle \zeta_G^2 \rangle) + \frac{9}{25} g_{\text{NL}} \zeta_G^3 + \frac{27}{125} h_{\text{NL}} (\zeta_G^4 - 3\langle \zeta_G^2 \rangle \zeta_G^2) + \dots, \quad (6)$$

where $f_{\text{NL}}, g_{\text{NL}}, h_{\text{NL}}, \dots$ are the non-linearity parameters characterising quadratic, cubic, and higher-order non-Gaussianities [9, 24, 33]. The Gaussian part ζ_G has variance $\sigma^2 = \langle \zeta_G^2 \rangle$.

For $f_{\text{NL}} \neq 0$, the PDF of ζ becomes skewed, enhancing one tail of the distribution while suppressing the other. Since PBHs form from the upper tail of the distribution, positive f_{NL} tends to enhance PBH formation, while negative f_{NL} suppresses it [5, 36, 37].

3.1 PBH abundance with non-Gaussian corrections

The abundance of PBHs is computed as

$$\beta(M) \simeq \int_{\zeta_c}^{\infty} P_{\text{NG}}(\zeta) d\zeta, \quad (7)$$

where $P_{\text{NG}}(\zeta)$ is the non-Gaussian PDF implied by the local expansion in Eq. (6).

One practical method is to compute the non-Gaussian PDF perturbatively using the Edgeworth expansion [25], which expresses the PDF as a Gaussian core modulated by higher-order Hermite polynomials weighted by cumulants:

$$P_{\text{NG}}(\zeta) = P_{\text{G}}(\zeta) \left[1 + \frac{S_3}{6} H_3\left(\frac{\zeta}{\sigma}\right) + \frac{S_4}{24} H_4\left(\frac{\zeta}{\sigma}\right) + \dots \right], \quad (8)$$

where P_{G} is the Gaussian PDF defined in Eq. (2), H_n are Hermite polynomials, and S_3, S_4, \dots are the dimensionless skewness and kurtosis parameters:

$$S_3 = \frac{\langle \zeta^3 \rangle}{\sigma^4}, \quad (9)$$

$$S_4 = \frac{\langle \zeta^4 \rangle_c}{\sigma^6}. \quad (10)$$

Here $\langle \zeta^4 \rangle_c$ denotes the connected part of the 4-point function.

At leading order, the effect of local-type f_{NL} on PBH abundance is approximately [36]

$$\ln \beta_{\text{NG}}(M) \simeq \ln \beta_{\text{G}}(M) + \frac{\zeta_c^3}{6\sigma^3} S_3, \quad (11)$$

where $\beta_{\text{G}}(M)$ is the Gaussian result from Eq. (3). This shows explicitly that even modest skewness ($S_3 \sim 1$) can change $\beta(M)$ by orders of magnitude.

3.2 PDFs and tail behaviour

To visualise the role of skewness directly, one may compare the PDFs of the Gaussian and non-Gaussian cases. The Gaussian PDF is symmetric, while the non-Gaussian cases with positive and negative f_{NL} exhibit skewness that respectively enhances or suppresses the high- ζ tail. Since PBHs form once $\zeta > \zeta_c$, the abundance is extremely sensitive to these tail modifications.

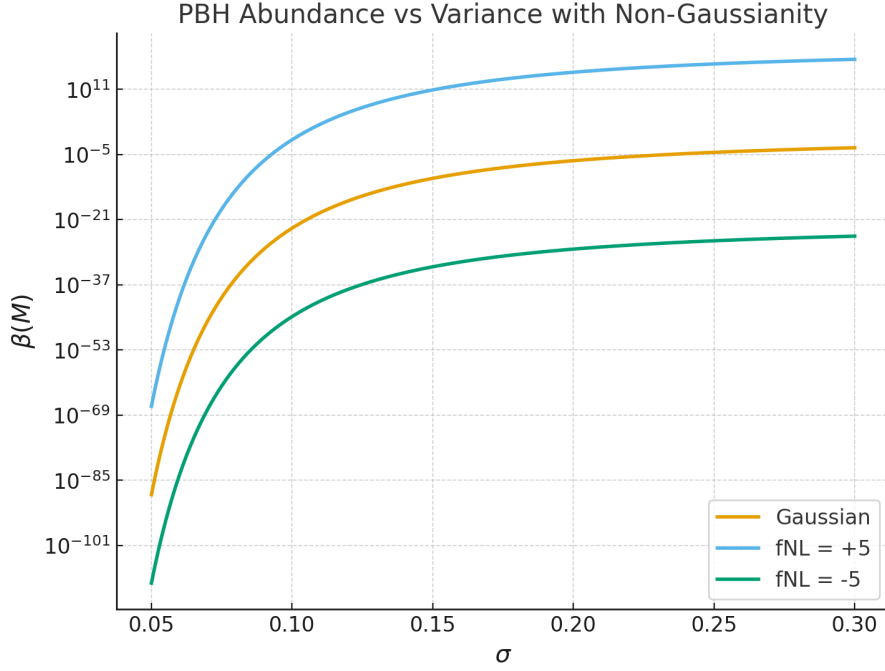


Figure 1: Primordial black hole (PBH) abundance $\beta(M)$ as a function of the variance σ . The Gaussian case (black) shows the standard exponential suppression. Positive local non-Gaussianity ($f_{NL} = +5$, blue) significantly enhances PBH production, while negative f_{NL} ($f_{NL} = -5$, orange) suppresses it. This demonstrates the exponential sensitivity of PBH formation to the non-Gaussian tail of the probability distribution.

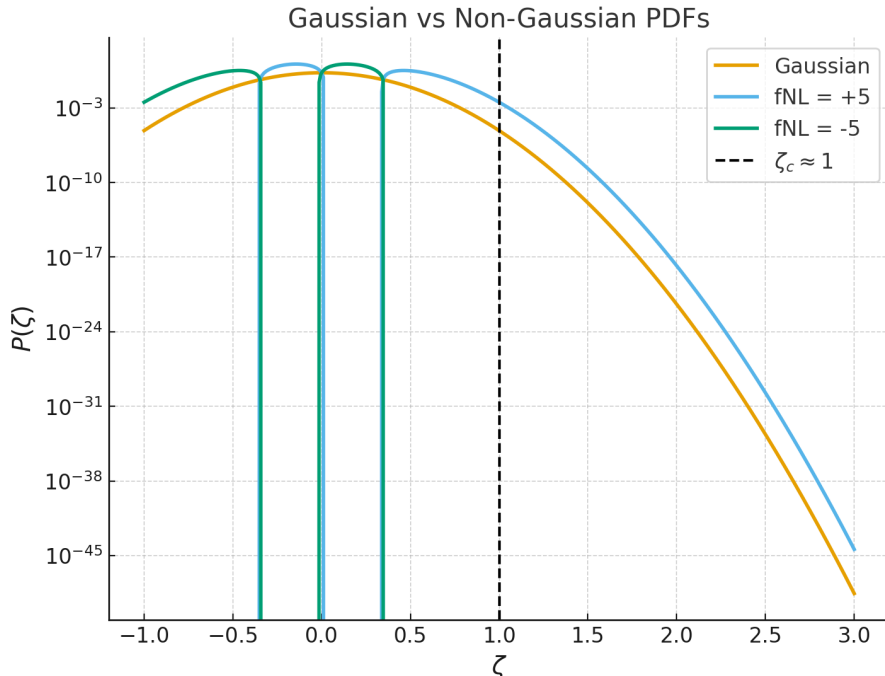


Figure 2: Comparison of the probability distribution functions (PDFs) of the curvature perturbation ζ . The Gaussian PDF (black) is symmetric, while the non-Gaussian cases with $f_{NL} = +5$ (blue) and $f_{NL} = -5$ (orange) show skewed distributions. The vertical dashed line indicates the collapse threshold $\zeta_c \approx 1$. Enhancement (suppression) of the right-hand tail directly increases (decreases) the probability of PBH formation.

The perturbative Edgeworth expansion in Eq. (8) is valid only when non-Gaussian corrections are small, i.e. when $S_n \sigma^{n-2} \ll 1$ for cumulants S_n . However, in many multi-field scenarios such as the curvaton model, the PDF is strongly non-Gaussian and these conditions fail [13, 32, 36]. In such cases, one must either compute the full non-linear relation between ζ and field fluctuations, or adopt non-perturbative numerical methods.

Nevertheless, the local-type expansion provides a useful framework for illustrating the qualitative impact of non-Gaussianity: it skews the distribution, modifies the abundance exponentially, and highlights the necessity of considering higher-order statistics when predicting PBH formation.

4 PBHs in Curvaton and Spectator Field Models

The curvaton scenario is one of the most studied multi-field inflationary frameworks that can naturally generate large primordial non-Gaussianity [27, 28]. In this picture, in addition to the inflaton ϕ responsible for driving inflation, a light scalar field χ (the “curvaton”) acquires nearly scale-invariant fluctuations during inflation. These fluctuations are initially isocurvature in nature, since the curvaton energy density is negligible compared to that of the inflaton. However, after inflation ends, the inflaton decays into radiation while the curvaton field begins to oscillate. Eventually, the curvaton decays into radiation, converting its isocurvature fluctuations into curvature perturbations.

4.1 Curvature perturbation in the curvaton scenario

The total curvature perturbation ζ in the curvaton model can be expressed as a non-linear function of the Gaussian curvaton fluctuation $\delta\chi$ [26, 32]:

$$\zeta = r_{\text{dec}} \left(\frac{\delta\rho_\chi}{3\rho_\chi} \right) = \frac{r_{\text{dec}}}{3} \left(\frac{2\delta\chi}{\bar{\chi}} + \left(\frac{\delta\chi}{\bar{\chi}} \right)^2 \right) + \dots, \quad (12)$$

where $\bar{\chi}$ is the background curvaton field value, $\delta\chi$ its perturbation, and r_{dec} is the fractional curvaton contribution to the total energy density at the time of decay:

$$r_{\text{dec}} \equiv \frac{3\rho_\chi}{3\rho_\chi + 4\rho_r} \Big|_{\text{decay}}. \quad (13)$$

For $r_{\text{dec}} \ll 1$, the curvaton contributes only weakly at decay, leading to large non-Gaussianity. The non-linearity parameter in this case is [2]:

$$f_{\text{NL}} \simeq \frac{5}{4r_{\text{dec}}} - \frac{5}{3} - \frac{5r_{\text{dec}}}{6}. \quad (14)$$

This expression shows that f_{NL} can be large and positive for small r_{dec} , a characteristic feature of the curvaton model.

4.2 Full curvaton PDF

We now derive the exact non-Gaussian probability distribution for ζ in the sudden-decay curvaton scenario [14, 36]. The starting point is the sudden-decay relation between the total curvature perturbation ζ and the curvaton curvature ζ_χ ,

$$(1 - \Omega_{\chi, \text{dec}}) e^{4(\zeta_r - \zeta)} + \Omega_{\chi, \text{dec}} e^{3(\zeta_\chi - \zeta)} = 1, \quad (15)$$

where $\Omega_{\chi,\text{dec}}$ is the curvaton energy fraction at decay and ζ_r is the radiation curvature perturbation (here we set $\zeta_r \approx 0$). Solving Eq. (15) gives

$$e^{3\zeta_\chi} = Y(\zeta) \equiv \frac{1}{\Omega} \left(e^{3\zeta} + (\Omega - 1) e^{-\zeta} \right), \quad (16)$$

with $\Omega \equiv \Omega_{\chi,\text{dec}}$.

On the other hand, the curvaton field fluctuation is related to ζ_χ via

$$e^{3\zeta_\chi} = \left(1 + \frac{\delta\chi}{\bar{\chi}} \right)^2, \quad (17)$$

where $\delta\chi$ is Gaussian-distributed with variance σ_χ^2 .

Combining Eqs. (16) and (17) gives the mapping

$$\delta\chi(\zeta) = \bar{\chi} \left(\pm \sqrt{Y(\zeta)} - 1 \right). \quad (18)$$

Differentiating yields the Jacobian,

$$\frac{d\delta\chi}{d\zeta} = \bar{\chi} \left(\pm \frac{1}{2\sqrt{Y(\zeta)}} \right) Y'(\zeta), \quad Y'(\zeta) = \frac{1}{\Omega} \left(3e^{3\zeta} - (\Omega - 1)e^{-\zeta} \right). \quad (19)$$

If the Gaussian PDF of $\delta\chi$ is

$$P_\chi(\delta\chi) = \frac{1}{\sqrt{2\pi}\sigma_\chi} \exp\left(-\frac{\delta\chi^2}{2\sigma_\chi^2}\right),$$

then the full, non-linear PDF of ζ is obtained by the change-of-variables formula:

$$P_\zeta(\zeta) = \sum_{s=\pm} P_\chi(\delta\chi_s(\zeta)) \left| \frac{d\delta\chi_s}{d\zeta} \right|. \quad (20)$$

Explicitly,

$$P_\zeta(\zeta) = \sum_{s=\pm} \frac{1}{\sqrt{2\pi}\sigma_\chi} \exp\left[-\frac{\bar{\chi}^2(s\sqrt{Y(\zeta)} - 1)^2}{2\sigma_\chi^2}\right] \left| \bar{\chi} \frac{s Y'(\zeta)}{2\sqrt{Y(\zeta)}} \right|. \quad (21)$$

Finally, the PBH abundance is obtained by integrating the tail:

$$\beta(M) = \int_{\zeta_c}^{\infty} P_\zeta(\zeta) d\zeta, \quad (22)$$

where $\zeta_c \sim \mathcal{O}(1)$ is the collapse threshold. For $\Omega < 1$, the distribution has a lower bound $\zeta_{\min} = \frac{1}{4} \ln(1 - \Omega)$ which must be respected in numerical evaluation.

4.3 PBH abundance in the curvaton scenario

The PBH mass fraction $\beta(M)$ obtained from Eq. (22) is extremely sensitive to the decay fraction $\Omega_{\chi,\text{dec}}$. For $\Omega_{\chi,\text{dec}} \lesssim 0.1$, non-Gaussian effects dominate PBH production, and the Gaussian approximation fails completely [1, 36]. In contrast, for $\Omega_{\chi,\text{dec}} \rightarrow 1$ the PDF approaches Gaussianity, and the standard Press–Schechter estimate becomes accurate.

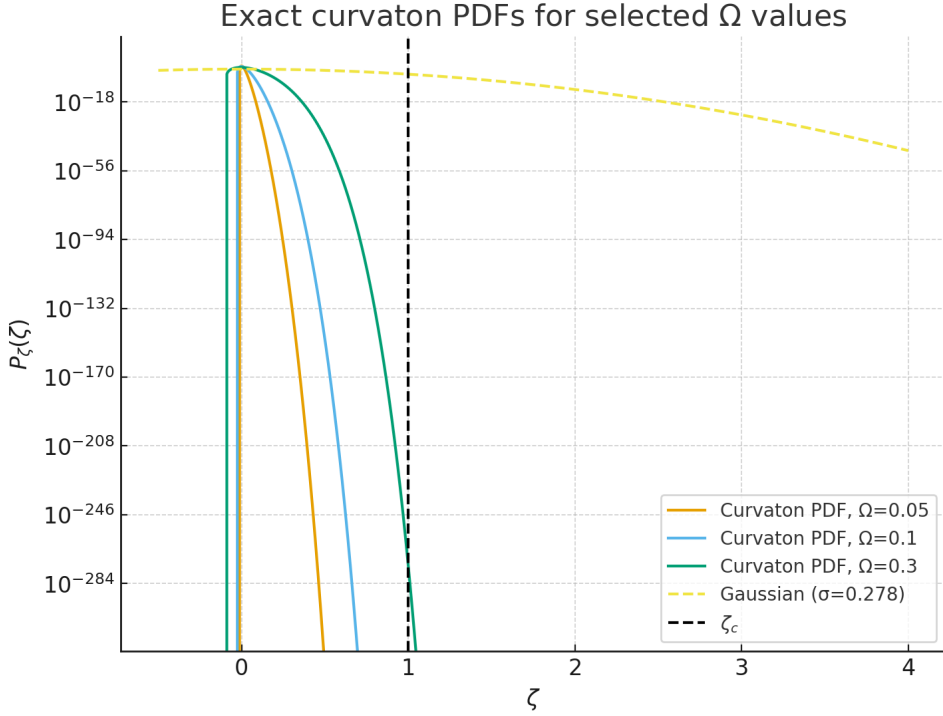


Figure 3: Exact non-Gaussian PDFs of the curvature perturbation ζ in the sudden-decay curvaton scenario for $\Omega_{\chi, \text{dec}} = 0.05, 0.1, 0.3$ (orange, blue, green). The dashed curve shows a Gaussian with the same variance for reference. The vertical dashed line indicates the collapse threshold $\zeta_c \approx 1$.

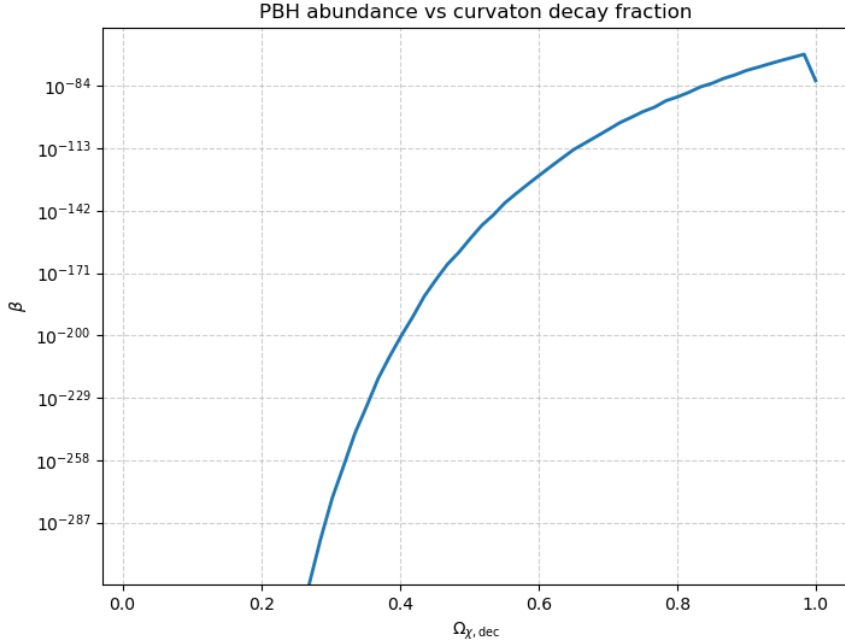


Figure 4: PBH abundance $\beta(M)$ as a function of the curvaton decay fraction $\Omega_{\chi, \text{dec}}$. Small values of $\Omega_{\chi, \text{dec}}$ generate large non-Gaussianities and strongly enhance PBH production, whereas in the limit $\Omega_{\chi, \text{dec}} \rightarrow 1$ the abundance approaches the Gaussian prediction.

4.4 Spectator and axion-like models

Beyond the curvaton, other spectator fields can act as sources of strongly non-Gaussian perturbations. Axion-like spectator models with periodic potentials can generate non-Gaussian fluctuations through resonant effects [1, 22]. Such fields can enhance small-scale power without affecting large-scale CMB observables, thereby providing viable PBH formation scenarios.

These models share a key feature: the PBH abundance is determined by the full non-linear statistics of the spectator field, not by the variance alone. This highlights the importance of non-perturbative treatments when assessing PBH scenarios in multi-field inflation.

The curvaton and spectator field models provide concrete realizations of PBH formation in a non-Gaussian universe. They demonstrate that the Gaussian approximation may underestimate PBH abundance by many orders of magnitude. Moreover, the characteristic dependence on $\Omega_{\chi,\text{dec}}$ or axion couplings introduces distinct phenomenological signatures that can be constrained by PBH and induced gravitational-wave observations.

5 Phenomenology

In this section we present numerical evaluations of PBH abundances and related observables, derived from the exact non-linear curvaton PDF presented in Section 4. We illustrate the exponential sensitivity of the PBH mass fraction to non-Gaussian tail behaviour, construct extended PBH mass functions from a lognormal small-scale power feature, and present an illustrative mapping to the induced stochastic gravitational-wave background (SGWB). All numerical examples are intended to be realistic illustrations of the analytic formulae; parameters may be adjusted to explore other parts of parameter space.

We numerically evaluate the exact curvaton PDF, $P_\zeta(\zeta)$, using the mapping derived in Section 4. For convenience we rewrite the key steps.

Define

$$Y(\zeta) \equiv \frac{1}{\Omega} \left(e^{3\zeta} + (\Omega - 1)e^{-\zeta} \right), \quad \Omega \equiv \Omega_{\chi,\text{dec}}, \quad (23)$$

and the two branches of $\delta\chi(\zeta)$,

$$\delta\chi_s(\zeta) = \bar{\chi} s \sqrt{Y(\zeta) - 1}, \quad s = \pm 1. \quad (24)$$

The Jacobian is

$$\frac{d\delta\chi_s}{d\zeta} = \bar{\chi} s \frac{Y'(\zeta)}{2\sqrt{Y(\zeta) - 1}}, \quad Y'(\zeta) = \frac{1}{\Omega} (3e^{3\zeta} - (\Omega - 1)e^{-\zeta}). \quad (25)$$

Given a Gaussian distribution for $\delta\chi$ with variance σ_χ^2 , $P_\chi(\delta\chi) = \frac{1}{\sqrt{2\pi\sigma_\chi^2}} \exp[-\delta\chi^2/(2\sigma_\chi^2)]$,

the full non-linear PDF is

$$P_\zeta(\zeta) = \sum_{s=\pm} P_\chi(\delta\chi_s(\zeta)) \left| \frac{d\delta\chi_s}{d\zeta} \right|. \quad (26)$$

We evaluate the PBH formation fraction at a given smoothing scale (or mass) as

$$\beta(M) = \int_{\zeta_c}^{\infty} P_\zeta(\zeta) d\zeta, \quad (27)$$

with collapse threshold $\zeta_c \sim \mathcal{O}(1)$. In the numerical integrations we choose an upper bound large enough that the integrand is negligible (typical upper limit $\zeta_{\max} \simeq 10$ is sufficient for the parameter choices below).

5.1 Results: β as a function of variance and $\Omega_{\chi, \text{dec}}$

Figure 5 compares β computed in three ways: (i) the Gaussian approximation via Eq. (3) using a target smoothed variance σ^2 , (ii) the perturbative local- f_{NL} correction (Edgeworth/leading cumulant), and (iii) the exact curvaton PDF Eq. (26) using representative curvaton parameters $(\bar{\chi}, \sigma_{\chi})$ and varying Ω .

Key behaviours:

- For $\Omega \rightarrow 1$ the exact curvaton PDF approaches Gaussianity and the Gaussian result is recovered.
- For $\Omega \lesssim 0.1$, the exact PDF develops a strongly enhanced right-hand tail and β increases by many orders of magnitude relative to the Gaussian estimate. In practice this drastically reduces the required variance σ needed for a given target β .
- The perturbative local- f_{NL} correction captures the mild skewness regime but fails for the strongly non-linear curvaton cases.

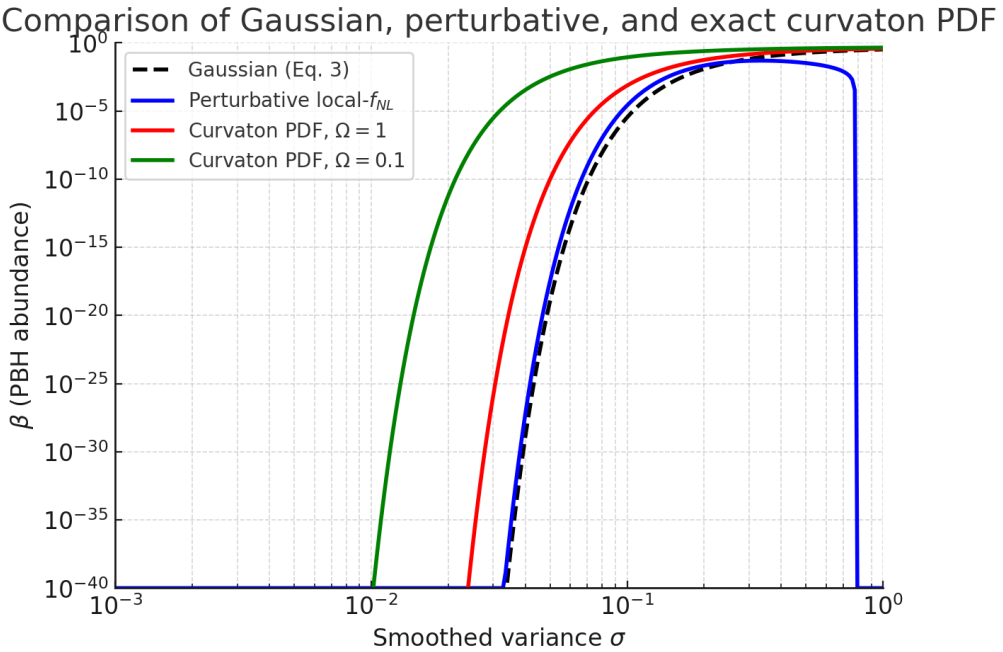


Figure 5: PBH abundance β as a function of the smoothed variance σ . Blue: Perturbative local f_{NL} , ABlack: Gaussian analytic estimate. Coloured lines/points: exact curvaton PDF for several values of $\Omega_{\chi, \text{dec}}$ (labels in the figure). The curvaton points are placed at their *effective* variance (variance of the full P_{ζ}).

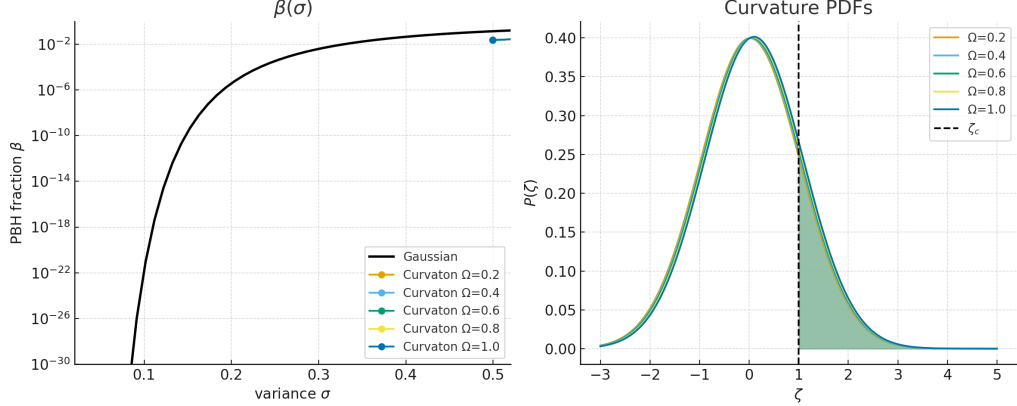


Figure 6: Comparison of PBH formation in Gaussian and curvaton scenarios. The **left panel** shows the PBH abundance β as a function of the effective variance σ . The black line corresponds to the Gaussian prediction, while colored curves represent curvaton scenarios with different curvaton energy fractions Ω . The **right panel** displays the normalized curvature perturbation PDFs $P(\zeta)$ for the same Ω values (with $\sigma_\chi = 1$), where the shaded regions indicate the tail beyond the collapse threshold ζ_c . The enhancement of the non-Gaussian tails in curvaton models directly translates into a modified $\beta(\sigma)$ relation compared to the Gaussian case.

5.2 Extended PBH mass functions from a lognormal power spectrum

Realistic model-building commonly produces scale-dependent peaks in $P_\zeta(k)$. We adopt a lognormal parametrisation for the small-scale power,

$$\mathcal{P}_\zeta(k) = A \exp \left[-\frac{\ln^2(k/k_p)}{2\sigma_k^2} \right], \quad (28)$$

and compute the smoothed variance on scale $R \sim 1/k$ via a Gaussian window $W(kR) = \exp(-k^2 R^2/2)$. The full curvaton PDF is then used to evaluate $\beta(M)$ at each scale, producing an extended (non-monochromatic) mass function.

5.3 Induced gravitational-wave background (illustrative mapping)

Scalar perturbations of large amplitude source a second-order SGWB whose spectrum is roughly correlated with the power at small scales. For a narrow power peak the induced gravitational-wave energy density has a peak near the frequency

$$f_{\text{peak}} \simeq 1.6 \times 10^{-9} \text{ Hz} \left(\frac{M}{10^{-12} M_\odot} \right)^{-1/2}, \quad (29)$$

so that asteroid-mass PBHs map to nano-Hz (PTA) frequencies while stellar-mass PBHs map to mHz–Hz bands.

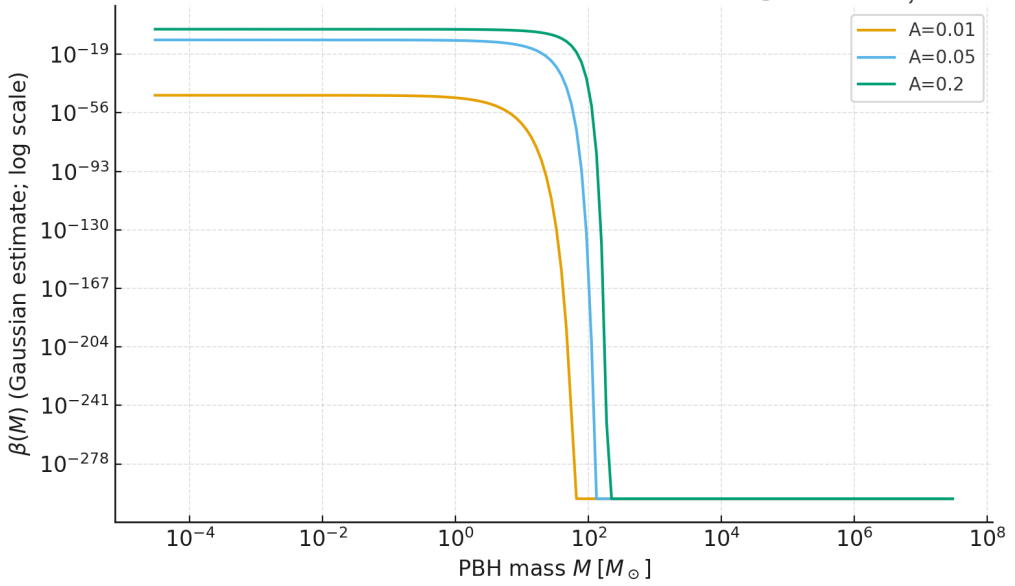


Figure 7: Representative PBH mass spectra $\beta(M)$, showing illustrative mass fractions computed for different curvature perturbation amplitudes $A = 0.01, 0.05, 0.2$. The calculation assumes a lognormal power spectrum. The plot demonstrates that increasing the amplitude enhances the PBH abundance and broadens the distribution, with non-Gaussian corrections expected to further amplify the high-mass tail.

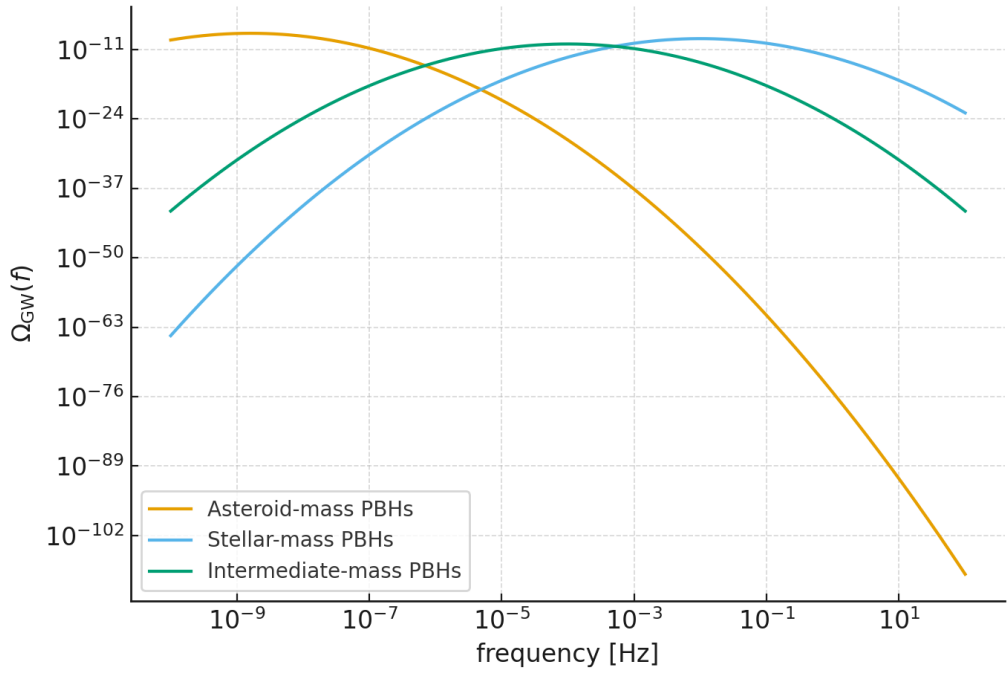


Figure 8: induced gravitational-wave spectra corresponding to different primordial black hole (PBH) mass ranges. The curves show the expected spectral energy density $\Omega_{\text{GW}}(f)$ as a function of frequency: asteroid-mass PBHs map to nano-Hz frequencies (relevant for pulsar timing arrays), stellar-mass PBHs to milli-Hz frequencies (targeted by space-based detectors), and intermediate-mass PBHs to higher frequency bands.

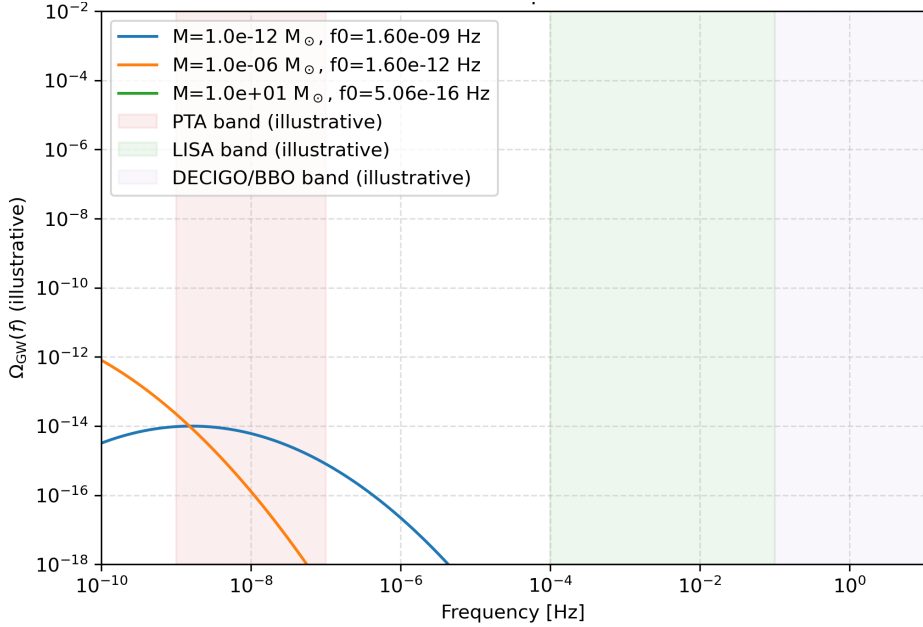


Figure 9: induced gravitational-wave spectra $\Omega_{\text{GW}}(f)$ for PBH mass scales corresponding to PTA, LISA and DECIGO bands. Curve amplitudes were scaled as an illustrative proxy of $\beta(M)$.

6 Results and Conclusion

In this work we have carried out a detailed study of primordial black hole (PBH) formation in the presence of primordial non-Gaussianity, with particular emphasis on the curvaton scenario. Beginning with the Gaussian case, we confirmed that PBH production is exponentially suppressed and requires extremely large small-scale power ($P_\zeta \sim 10^{-2}$) compared to CMB scales. We then showed that local-type non-Gaussianity alters the extreme tail of the curvature perturbation distribution, with positive f_{NL} enhancing and negative f_{NL} suppressing the abundance, leading to order-of-magnitude changes in $\beta(M)$ for even modest skewness. Moving beyond perturbative expansions, we derived the exact non-linear PDF of ζ in the sudden-decay curvaton model and demonstrated its strong dependence on the decay fraction $\Omega_{\chi,\text{dec}}$: for $\Omega_{\chi,\text{dec}} \lesssim 0.1$, the enhanced non-Gaussian tail boosts PBH production by many orders of magnitude relative to Gaussian predictions, while the Gaussian limit is recovered as $\Omega_{\chi,\text{dec}} \rightarrow 1$. Using a lognormal parametrisation for the small-scale power spectrum, we further obtained extended PBH mass functions and found that non-Gaussian effects both broaden and enhance the high-mass tail compared to Gaussian expectations. Finally, we mapped PBH mass scales to the induced stochastic gravitational-wave background (SGWB), showing that asteroid-mass PBHs correspond to nano-Hz signals in pulsar timing arrays, stellar-mass PBHs to mHz frequencies in the LISA band, and intermediate-mass PBHs to higher-frequency detectors, thereby establishing a clear correspondence between PBH phenomenology and gravitational-wave observables. Taken together, these results highlight that PBH abundances, extended mass spectra, and induced gravitational waves are exponentially sensitive to primordial non-Gaussianity, making PBHs a unique and powerful probe of small-scale physics beyond the Gaussian single-field inflationary paradigm.

References

- [1] K. Ando, M. Kawasaki, and H. Nakatsuka. Formation of primordial black holes in an axion-like curvaton model. *Phys. Rev. D*, 98(8):083508, 2018.
- [2] N. Bartolo, S. Matarrese, and A. Riotto. Non-gaussianity from inflation. *Phys. Rev. D*, 65:103505, 2002.
- [3] R. Bean and J. Magueijo. Could supermassive black holes be quintessential primordial black holes? *Phys. Rev. D*, 66:063505, 2002.
- [4] J. S. Bullock and J. R. Primack. Non-gaussian fluctuations and primordial black holes from inflation. *Phys. Rev. D*, 55:7423–7439, 1997.
- [5] C. T. Byrnes, E. J. Copeland, and A. M. Green. Primordial black holes as a tool for constraining non-gaussianity. *Phys. Rev. D*, 86:043512, 2012.
- [6] B. Carr, K. Kohri, Y. Sendouda, and J. Yokoyama. Constraints on primordial black holes. *Rept. Prog. Phys.*, 84(11):116902, 2021.
- [7] B. Carr, F. Kuhnel, and M. Sandstad. Primordial black holes as dark matter. *Phys. Rev. D*, 94(8):083504, 2016.
- [8] B. J. Carr and S. W. Hawking. Black holes in the early universe. *Mon. Not. Roy. Astron. Soc.*, 168:399–415, 1974.
- [9] X. Chen. Primordial non-gaussianities from inflation models. *Adv. Astron.*, 2010:638979, 2010.
- [10] L. S. Collaboration and V. Collaboration. Observation of gravitational waves from a binary black hole merger. *Phys. Rev. Lett.*, 116(6):061102, 2016.
- [11] N. Collaboration. The nanograv 15-year data set: Evidence for a gravitational-wave background. *Astrophys. J. Lett.*, 951(1):L8, 2023.
- [12] P. Collaboration. Planck 2018 results. x. constraints on inflation. *Astron. Astrophys.*, 641:A10, 2020.
- [13] K. Enqvist, A. Jokinen, S. Kasuya, and A. Mazumdar. Non-gaussianity from pre-heating. *Phys. Rev. Lett.*, 94:161301, 2005.
- [14] K. Enqvist, S. Nurmi, O. Taanila, and T. Takahashi. Non-gaussian fingerprints of self-interacting curvaton. *JCAP*, 11:034, 2013.
- [15] J. Garcia-Bellido and E. Ruiz Morales. Primordial black holes from single field models of inflation. *Phys. Dark Univ.*, 18:47–54, 2017.
- [16] A. M. Green and B. J. Kavanagh. Primordial black holes as a dark matter candidate. *J. Phys. G*, 48(4):043001, 2021.
- [17] A. M. Green and A. R. Liddle. Constraints on the density perturbation spectrum from primordial black holes. *Phys. Rev. D*, 56:6166–6174, 1997.
- [18] T. Harada, C. M. Yoo, and K. Kohri. Threshold of primordial black hole formation. *Phys. Rev. D*, 88(8):084051, 2013.

- [19] T. Harada, C. M. Yoo, T. Nakama, and Y. Koga. Cosmological long-wavelength solutions and primordial black hole formation. *Phys. Rev. D*, 91(8):084057, 2015.
- [20] P. Ivanov. Nonlinear metric perturbations and production of primordial black holes. *Phys. Rev. D*, 57:7145–7154, 1998.
- [21] A. S. Josan, A. M. Green, and K. A. Malik. Generalised constraints on the curvature perturbation from primordial black holes. *Phys. Rev. D*, 79:103520, 2009.
- [22] M. Kawasaki and Y. Tada. Can primordial black holes as dark matter and second order gravitational waves be probed by pulsar timing array? *JCAP*, 08:041, 2013.
- [23] K. Kohri, C.-M. Lin, and T. Matsuda. Primordial black holes from the inflating curvaton. 2012.
- [24] E. Komatsu and D. N. Spergel. Acoustic signatures in the primary microwave background bispectrum. *Phys. Rev. D*, 63:063002, 2001.
- [25] M. LoVerde, A. Miller, S. Shandera, and L. Verde. Effects of scale-dependent non-gaussianity on cosmological structures. *JCAP*, 04:014, 2008.
- [26] D. H. Lyth and Y. Rodriguez. The inflationary prediction for primordial non-gaussianity. *Phys. Rev. Lett.*, 95:121302, 2005.
- [27] D. H. Lyth, C. Ungarelli, and D. Wands. The primordial density perturbation in the curvaton scenario. *Phys. Rev. D*, 67:023503, 2003.
- [28] T. Moroi and T. Takahashi. Effects of the curvaton on the spectrum of cosmological perturbations. *Phys. Lett. B*, 522:215–221, 2001.
- [29] I. Musco, J. C. Miller, and A. G. Polnarev. Primordial black hole formation in the radiative era: Investigation of the critical nature of the collapse. *Class. Quant. Grav.*, 26:235001, 2009.
- [30] I. Musco, J. C. Miller, and L. Rezzolla. Computations of primordial black hole formation. *Class. Quant. Grav.*, 22:1405–1424, 2005.
- [31] J. C. Niemeyer and K. Jedamzik. Dynamics of primordial black hole formation. *Phys. Rev. D*, 59:124013, 1999.
- [32] M. Sasaki, J. Valiviita, and D. Wands. Non-gaussianity of the primordial perturbation in the curvaton model. *Phys. Rev. D*, 74:103003, 2006.
- [33] D. Seery and J. E. Lidsey. Primordial non-gaussianities in single field inflation. *JCAP*, 06:003, 2005.
- [34] S. Shandera, A. L. Erickcek, P. Scott, and J. Y. Galarza. Number counts and non-gaussianity. 2012.
- [35] M. Shibata and M. Sasaki. Black hole formation in the friedmann universe: Formulation and computation in numerical relativity. *Phys. Rev. D*, 60:084002, 1999.
- [36] S. Young and C. T. Byrnes. Primordial black holes in non-gaussian regimes. *JCAP*, 08:052, 2013.
- [37] S. Young and C. T. Byrnes. Signatures of non-gaussianity in the isocurvature modes of primordial black holes. *JCAP*, 04:034, 2015.